Flexible polyelectrolyte simulations at the Poisson–Boltzmann level: A comparison of the kink-jump and multigrid configurational-bias Monte Carlo methods

Stefan Tsonchev[a)] and Rob D. Coalson
Department of Chemistry, University of Pittsburgh, Pittsburgh, Pennsylvania 15260

Anping Liu and Thomas L. Beck
Department of Chemistry, University of Cincinnati, Cincinnati, Ohio 45221

We present a new approach for simulating the motions of flexible polyelectrolyte chains based on the continuous kink-jump Monte Carlo technique coupled to a lattice field theory based calculation of the Poisson–Boltzmann (PB) electrostatic free energy ''on the fly.'' This approach is compared to the configurational-bias Monte Carlo technique, in which the chains are grown on a lattice and the PB equation is solved for each configuration with a linear scaling multigrid method to obtain the many-body free energy. The two approaches are used to calculate end-to-end distances of charged polymer chains in solutions with varying ionic strengths and give similar numerical results. The configurational-bias Monte Carlo/multigrid PB method is found to be more efficient, while the kink-jump Monte Carlo method shows potential utility for simulating nonequilibrium polyelectrolyte dynamics. © *2004 American Institute of Physics.* [DOI: 10.1063/1.1701841]

I. INTRODUCTION

Polyelectrolyte chains present many theoretical challenges due to the wide range of length scales which influence their structure and dynamics in condensed phase solutions.[1] These charged polymers figure prominently in both biophysical and technological applications. The chains can be either rather rigid (DNA) or highly flexible (poly-acrylate or NaPSS). Quantities which impact the equilibrium properties of the chain include charge density along the chain, ionic strength of the solvent, solvent dielectric constant, and segment excluded volume size. Recent theoretical work on flexible chains has focused on self-consistent field theories[2–4] and molecular level simulations. Simulation research has either been at the all-atom restricted primitive model level[5,6] or has utilized effective Debye–Hückel pair potentials.[7,8] In the present work, we adopt an intermediate strategy by modeling the polymer chains as discrete and treating the counterions and any added salt at the continuum Poisson–Boltzmann (PB) level.

Treating the background ions at the continuum level is a kind of Born–Oppenheimer approximation for the ion gas. It assumes that the background ions equilibrate much more quickly than the polymer chains, and allows for highly efficient sampling on the PB free energy surface. Previous simulations have employed similar approaches for rigid colloidal systems.[9–11]

The linearized Debye–Hückel theory is only strictly appropriate for very small potentials.[10] Generally, for charged polymers, this condition is not met in the region near the chain. The linearized theory fails to capture the nonlinear counterion condensation effect which occurs in water for singly charged counterions when the charge separation is less than 7.12 Å;[12] however, the nonlinear PB equation is known to properly account for the ion condensation at a semiquantitative level, at least for monovalent counterions and salt.[13,14] This condensation can have profound effects on the equilibrium structure of the chains.

In the present paper we apply the kink-jump Monte Carlo (KJMC) and the multigrid configurational bias Monte Carlo (CBMC) methods to the problem of calculating end-to-end distances of free charged polymer chains in electrolyte solutions of varying ionic strengths. Results of the two methods are compared to each other and to analogous calculations done at the Debye–Hückel (DH) level. Also, the relative efficiency of the two approaches is estimated. A long term goal of this work is to simulate large charged polymer systems without explicit inclusion of the ion gas and in a way which scales linearly with system size.

In Sec. II we describe the KJMC simulations for solving the PB equation ''on the fly.'' Then in Sec. III we discuss the CBMC method for sampling polymer configurations and the multigrid (MG) technique for solving the PB equation. Simulation results obtained via both methods are compared in Sec. IV, where we plot the equilibrium end-to-end distance of the charged chain as a function of the Debye length (i.e., ionic strength of the solution) and the monomer charge. Discussion and conclusions are provided in Sec. V.

II. MONTE CARLO SIMULATIONS WITH POISSON–BOLTZMANN CALCULATION OF THE ELECTROSTATIC FREE ENERGY "ON THE FLY"

The first Monte Carlo method we will employ is based on the kink-jump technique developed by Baumgärtner and

---

a)Present address: Department of Chemistry, Northwestern University, Evanston, IL 60208. Electronic mail: stefan@chem.northwestern.edu

Binder,[15] and later used by us to perform Monte Carlo simulations for calculation of partition coefficients of a polymer chain distributed among cavities with different sizes.[16] This method treats the polymer chain as a "pearl-necklace" in which two consecutive monomers are connected by a rigid rod of length l_0. The monomers are modeled as hard spheres whose radius is adjusted to describe the strength of the excluded volume interaction. Initially, the chain is placed at random in the simulation box. Then the chain motion is evolved by the kink-jump technique, where at each step a monomer, say the nth one, is picked at random and rotated around the axis connecting the $(n-1)$th and the $(n+1)$th monomers by a random angle. If the end monomer is chosen, it is moved to a new random position keeping the rod length between it and the monomer to which it is connected fixed.

After each monomer move, the polymer chain is put on a discrete lattice so that each monomer is placed on the nearest lattice point to its continuous coordinates. If the lattice spacing is l, and each point on a cubic lattice is described by the integer triple $\boldsymbol{n}$, then the discretized PB equation reads

$$\alpha \sum_m \Delta_{nm} \bar{\phi}_m = \gamma_+ \exp(\bar{\phi}_n - V_n) - \gamma_- \exp(-\bar{\phi}_n - V_n)$$

$$+ \sum_j Q_j \delta_{n,R_j}, \tag{1}$$

where Δ_{nm} is the lattice Laplacian,[17] $\alpha \equiv \epsilon l / 4\pi \beta q^2$ with ϵ the dielectric constant, $\beta = 1/kT$ the inverse temperature and q the proton charge; furthermore; Q_j is the charge of the jth monomer (in units of the proton charge), located at $\boldsymbol{R}_j$. This set of difference equations can be solved numerically using several methods. Here we employ a variational minimization strategy, as described in Ref. 17. As discussed at length in that work, the field $\{\bar{\phi}_n\}$ in Eq. (1) can be obtained as the unique minimum of a certain functional of lattice field variables. To locate this minimum, we employ a simple line minimization strategy with a Newton–Raphson routine to find the (unique) minimum in each successive field direction.[18] Given $\{\bar{\phi}_n\}$ satisfying Eq. (1), i.e., the dimensionless PB field (see below), the electrostatic free energy can be extracted via the relationship:[9,17,19]

$$\beta A = -\Xi_{mf} + n_+ \ln \gamma_+ + n_- \ln \gamma_-, \tag{2}$$

with

$$\Xi_{mf} = -\gamma_+ \sum_n \frac{\bar{\phi}_n}{2} \exp(\bar{\phi}_n - V_n) + \gamma_- \sum_n \frac{\bar{\phi}_n}{2}$$

$$\times \exp(-\bar{\phi}_n - V_n) + \sum_j Q_j \bar{\phi}_{R_j}/2. \tag{3}$$

In Eqs. (2) and (3), A is the Helmholtz free energy, $n_\pm$ is the number of $\pm$ (monovalent) mobile ions in the solution, V is an exclusion potential (which is zero in allowed regions of space and prohibitively high in forbidden regions), $\bar{\phi} = -\beta q \phi$ is the dimensionless electrostatic potential solving the PB equation, and $\gamma_\pm$ are determined by the condition

$$n_\pm = \gamma_\pm \sum_n e^{\pm \bar{\phi}_n - V_n}. \tag{4}$$

Moreover, the subscript "mf" stands for "mean field," and serves to remind us that Poisson–Boltzmann theory constitutes an approximation to the statistical mechanics of the mobile ion "gas." In the calculations presented here, we use fixed boundary conditions with the field ϕ set to zero at the boundary of the allowed region of space.

For each monomer move, δA, i.e., the difference between the electrostatic free energy of the chain before and after the trial move, is calculated, and the move is accepted with probability $p=1$ if $\delta A < 0$ (i.e., A is lower in the trial state than in the initial state), and $p = \exp(-\beta \delta A)$ if $\delta A > 0$. In other words, we employ the standard Metropolis algorithm. Once a decision is made about whether to accept or reject the trial configuration, the output configuration is returned to its original location in continuous three dimensional space and the next KJMC move is attempted.

III. CONFIGURATIONAL BIAS MONTE CARLO METHOD AND THE MULTIGRID TECHNIQUE FOR SOLVING THE POISSON–BOLTZMANN EQUATION

The strategy of this Monte Carlo method is to first grow the chains with a biased random walk using the CBMC approach.[20] This step is performed at the linearized pair potential level

$$\frac{v_{DH}(r)}{kT} = Z^2 \lambda_B \frac{e^{-\kappa r}}{r}. \tag{5}$$

Here Z is the monomer charge (in units of the proton charge), λ_B is the Bjerrum length and κ is the inverse Debye screening length, which depends on the electrolyte concentration. The linearized potential provides a guiding potential for the construction of the full chain. Then, we numerically solve the nonlinear PB equation with a multigrid technique (see below) to obtain a correction to the linearized energy entering into the Monte Carlo weight. The chain growth process is efficient and tends to direct the trial configuration into favorable regions. The correction factor modifies the trial weight with a Boltzmann factor resulting from the difference between the linearized and many-body free energies. One solution of the PB equation is thus required for each trial conformation. We emphasize that the simulation is conducted on the full Poisson–Boltzmann free energy surface and the linearized potential is only used to guide in the rapid growth of the trial conformation.

The CBMC method is described in detail in Ref. 20. To summarize, the chain is grown segment by segment, with the new segment location chosen based on its Boltzmann weight. The "local partition function" is then computed and the product of these terms during the growth process yields the Rosenbluth weight $W_{\Gamma'}$ for the trial conformation. The Monte Carlo choice is obtained simply from the ratio of the new and old Rosenbluth weights (in our case modified by the difference between the linearized energy and the many-body PB free energy, below). The CBMC technique is highly efficient, allowing for simulations of chains with hundreds of segments. The final Monte Carlo decision process with the nonlinear correction is

J. Chem. Phys., Vol. 120, No. 20, 22 May 2004

Flexible polyelectrolyte simulations   9819

$$P_{acc}(\Gamma \to \Gamma') = \text{Min}\left(1, \frac{W_{\Gamma'}e^{-\beta\Delta U_{\Gamma'}}}{W_{\Gamma}e^{-\beta\Delta U_{\Gamma}}}\right), \qquad (6)$$

where ΔU_{Γ} is the difference between the many-body and pair potential free energies. The majority of the time in this algorithm is spent in the numerical solution of the PB equation over the grid domain. In our simulations, we cut the chains at a random location and regrow the chain from the point of the cut with the above procedure. The advantages of the CBMC approach are (1) each regrowth process generates an independent trial configuration, (2) due to the nature of the growth process, the simulation efficiently samples large-amplitude motions, and (3) the PB equation only needs to be solved once per independent trial conformation.

We numerically solve the PB equation on a lattice using the full approximation scheme (FAS) MG method. The MG technique allows for solution of nonlinear problems with similar efficiency to linear ones, and it scales linearly in computer time with the system size. Details of our numerical approach are given in Refs. 14, 21, and 22. In the MG approach, the desired solution on the fine scale is corrected following iterations of a modified problem on coarser scales. These corrections decimate long wavelength components of the error which eliminates the "critical slowing down" problem occurring in real space solvers. The result is an algorithm that typically locates the solution in 10–20 lattice sweeps on the fine scale to within the truncation errors. In our work, we converged the total free energy to a small fraction of kT (0.01 kT).

IV. SIMULATION RESULTS AND DISCUSSION

We have applied the methods described in the previous sections to the calculation of the mean end-to-end distance, R, of a charged polymer chain in electrolyte solution. The chains in our calculations consist of 32 monomers, with a bond length of 4 Å which is chosen as the unit length in our plots. The motion of the chain is simulated in a cubic box of size 33^3, which is the same as the size of the lattice, that is, the lattice spacing is one bond length. In the KJMC simulation, after each move the chain is translated to the center of the box to ensure that it does not reach the end of the box and thus give rise to spurious edge effects. We have confirmed that the end-to-end distances resulting from the simulations of a noncharged chain under the same conditions satisfy all the proper theoretical predictions. Namely, in the case of no excluded volume interactions $R^2 = (N-1)$, and with excluded volume interactions $R^2 \cong (N-1)^{(6/5)}$ (with R measured in units of the bond length); in the 32 monomer case considered here, $R \cong 7.85$ when monomer excluded volume is "turned on."

The KJ and CBMC procedures considered in this paper represent the polymer configurations in somewhat different ways, as noted above. Again, the kink-jump model represents the polymer as beads connected by rods (in continuous space); excluded volume effects are included by giving the monomer beads a finite radius and disallowing any configurations where the finite-size beads overlap. On the other hand, the implementation of the CBMC method adopted in this work grows connected configurations on a cubic lattice.
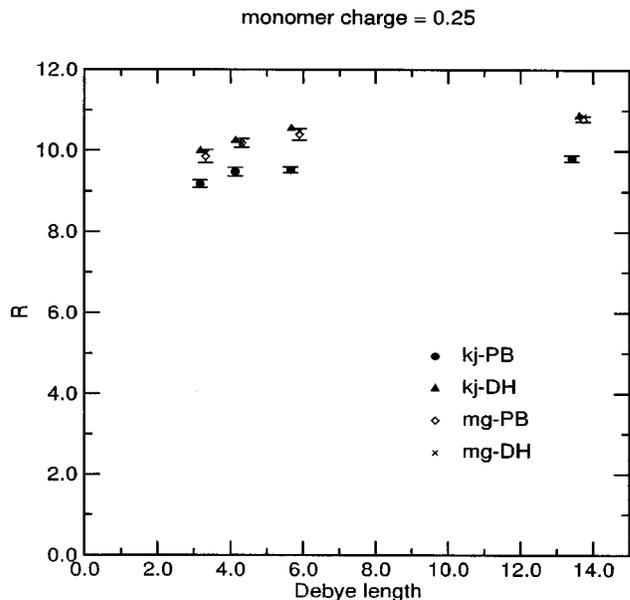
FIG. 1. The end-to-end distance R as a function of Debye length, both in units of bond length (4 Å), for a chain of 32 monomers, each having a charge of 0.25 (in units of the proton charge). The Debye lengths are averaged over the course of the simulation, and, in decreasing order, correspond to one, 20, 40, and 70 monovalent impurity ion pairs plus the appropriate number of monovalent negative counterions needed for electroneutrality of the solution; see text for further details. (The error bars for the Debye lengths, as well as for the Debye–Hückel results, are negligible and are, therefore, not shown.) The swelling of the chains due to the electrostatic repulsion between the charged monomers is evident, in comparison to the uncharged case for which $R \cong 7.85$. In the legend "kj" stands for results of the KJMC method, "mg" stands for the results of the multigrid CBMC techniques, "PB" stands for Poisson–Boltzmann, and "DH" stands for Debye–Hückel.

Excluded volume is enforced by forbidding a growing chain from visiting any lattice site that is already occupied.

In the long chain limit we expect the fine details of how equilibrium configurations of the polymer chain are sampled to become irrelevant, based on general principles such as the central limit theorem.[23] However, for modest length chains which can be accessed by explicit simulation, some differences in system properties due to the polymer model are inevitable. Since we are primarily interested here in electrostatic issues arising from the charge on the polymer chain and mobile ions in the solvent, we have attempted to generate the most meaningful comparison of the predictions of our two models by adjusting model parameters such that the properties of the *un*charged polymer systems agree. Then electrostatic effects are introduced, and the results obtained via both models are compared with no further parameter adjustment.

In particular, before the polyelectrolyte computations the two methods were calibrated by adjusting the excluded volume radius in the continuous kink-jump simulation so that it produces the same end-to-end distance as the multigrid CBMC method in the case of noncharged chains. The effective radius resulting from this calibration, and then used throughout in the kink-jump simulations, was 0.34 bond lengths.

In Fig. 1 we show the dependence of R on the Debye length for the case of a chain with monomer charge 0.25 (in
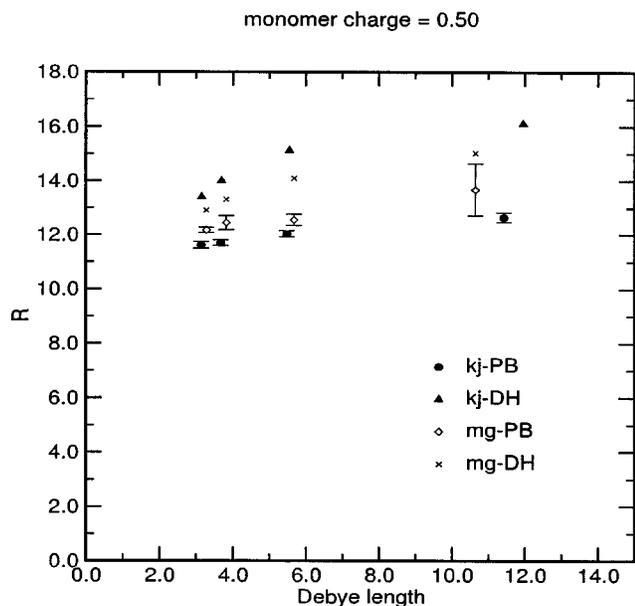
monomer charge = 0.50

FIG. 2. Same as Fig. 1 for monomer charge 0.50. The Debye lengths, in decreasing order, correspond to one, 20, 50, and 70 monovalent impurity ion pairs.

units of the proton charge). To achieve different Debye lengths, an appropriate number of monovalent impurity ion pairs was added into the solvent portion of the simulation box. (In addition, the number of monovalent negative counterions needed to neutralize the positive charge on the polymer chain was added to the solvent; in Fig. 1, this amounted to $32 \times 0.25 = 8$ such counterions.) Figures 2 and 3 present the corresponding results for R in the cases of monomer charge 0.50 and 0.75, respectively. Note that monomer charges 0.25,
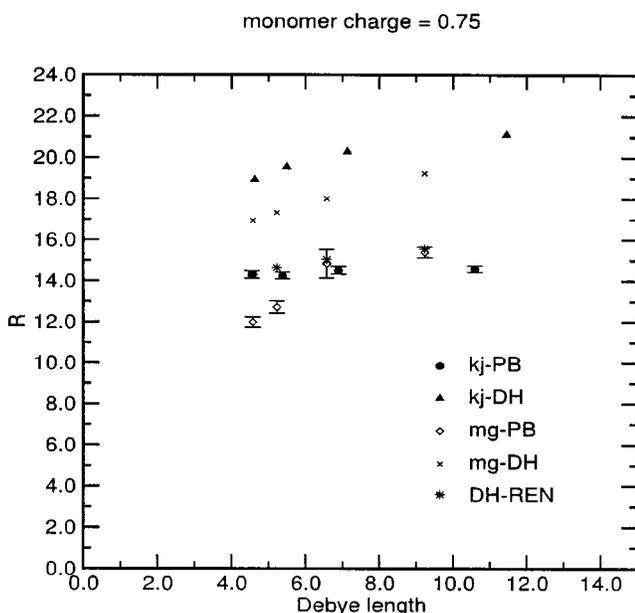
monomer charge = 0.75

FIG. 3. Same as Fig. 1 for monomer charge 0.75. The Debye lengths, in decreasing order, correspond to one, ten, 20, and 30 monovalent impurity ion pairs. DH-REN indicates results of a simulation based on a Debye–Hückel pair potential with renormalized monomer charge; see text for details. (It should be noted that the results for kj-PB and DH-REN in the case of 30 monovalent impurity ions are nearly coincident.)

0.50, and 0.75 correspond to 15.5, 7.75, and 5.17 Å between charges if we had put unit charges on the chain. The onset of condensation occurs at a chain charge density of one (proton) charge every 7.12 Å, so this set of figures shows how we approach and exceed that threshold. Both the KJMC and the multigrid CBMC simulations were performed for a water solution with a dielectric constant $\epsilon = 78$. Each figure shows KJMC and CBMC results based on an electrostatic free energy calculated at the PB level. For comparison, analogous results obtained by approximating the electrostatic free energy as a sum of Debye–Hückel pair potentials are also displayed.

In the case of small monomer charge, Fig. 1, we observe practically coinciding results from the multigrid CBMC simulation and both Debye–Hückel simulations, while the end-to-end distances resulting from the KJMC PB simulation are somewhat shorter. We believe this difference is due to an artifact of the (different) lattices used in the two types of calculation. Fortunately, the discrepancies do not exceed ~10% between corresponding KJMC and CMBC results in any of the figures, despite the relatively coarse lattices utilized to produce them. In Figs. 2 and 3, as the monomer charge increases, we observe a deviation between the Poisson–Boltzmann and the Debye–Hückel results, which is most obvious in Fig. 3, where the monomers have the relatively large charge of 0.75. In that case, the two PB simulations agree well with each other, perhaps because the chains are stretched due to the stronger intermonomer repulsion, making the more folded configurations less likely, and diminishing the effect of the lattice artifacts mentioned above. In Fig. 3 we also show via unfilled triangles (DH-REN) results based on a CBMC DH-level calculation in which the charge on the monomers has been renormalized to a value of 1 proton charge per 7.12 Å. According to Manning counterion condensation theory,[12] for chain charge densities exceeding this critical value, some counterions from the surrounding liquid condense onto the chain so as to reduce the effective polymer charge density to the critical value. The results obtained here are consistent with such a mechanism.

For the KJMC simulations we define 32 monomer moves (simulation steps), which on average correspond to one move per each monomer in the chain, as one simulation sweep. The number of simulation sweeps for the results presented here was between 120 000 and 180 000 per calculation. After computing the PB free energy on the lattice, we saved the old electrostatic field and used it as a starting field for the next computation. This significantly reduced the computation time, since in the kink-jump simulations we move only one monomer at a time, so that the new electrostatic field is only slightly perturbed from the old one. Thus, after the first PB computation on the lattice, we only needed between one and five iterations to find the new PB free energy within the same predetermined precision [based on the residual of the numerical solution of Eq. (1)]. For the CBMC PB simulations, the polymer chain was regrown 20 000 times in each run. In both the KJMC and the CBMC DH simulations 10^6 sweeps were performed.

V. DISCUSSION AND CONCLUSIONS

We have estimated that for the calculations presented here, the multigrid CBMC method is about 34 times more efficient than the kink-jump Monte Carlo method in terms of computational speed. A significant fraction of this speed-up can be attributed to use of a multigrid PB solver in the CBMC calculations. Such a solver can and should be implemented into further investigations of polyelectrolyte kinetics and statistical mechanics via the KJMC method. The latter method remains of interest, since it can be used to study nonequilibrium problems, e.g., in the area of biopolymer dynamics.[24] We expect that using a finer lattice in the simulations would alleviate the lattice artifacts encountered in the calculations presented here and would thus yield even better agreement between the two simulation techniques. The constantly improving capacities of modern computers will undoubtedly allow significantly finer lattices to be employed in the near future, thus enhancing the capability of both KJMC and CBMC techniques for dealing with a wide variety of problems involving polyelectrolyte solutions.

[1] J. L. Barrat and J. F. Joanny, Adv. Chem. Phys. **94**, 1 (1996).
[2] A. Yethiraj, J. Chem. Phys. **108**, 1184 (1998).
[3] J. P. Donley, J. Rudnick, and A. J. Liu, Macromolecules **30**, 1188 (1997).
[4] I. Borukhov, D. Andelman, and H. Orland, Eur. Phys. J. B **5**, 869 (1998).
[5] M. J. Stevens and K. Kremer, J. Phys. II **6**, 1607 (1996).
[6] M. J. Stevens and K. Kremer, J. Chem. Phys. **103**, 1669 (1995).
[7] M. Ullner, B. Jönsson, C. Peterson, O. Sommelius, and B. Söderberg, J. Chem. Phys. **107**, 1279 (1997).
[8] U. Micka and K. Kremer, J. Phys.: Condens. Matter **8**, 9463 (1996).
[9] A. M. Walsh and R. D. Coalson, J. Chem. Phys. **100**, 1559 (1994).
[10] M. Fushiki, J. Chem. Phys. **97**, 6700 (1992).
[11] H. Löwen, J. Chem. Phys. **100**, 6738 (1994).
[12] G. S. Manning, Q. Rev. Biophys. **11**, 179 (1978); Acc. Chem. Res. **12**, 443 (1979).
[13] G. V. Ramanathan, J. Chem. Phys. **78**, 3223 (1983).
[14] S. Tomac and A. Gräslund, J. Comput. Chem. **19**, 893 (1998).
[15] A. Baumgärtner and K. Binder, J. Chem. Phys. **71**, 2541 (1979).
[16] S. Tsonchev, R. D. Coalson, S.-S. Chern, and A. Duncan, J. Chem. Phys. **113**, 8381 (2000).
[17] R. D. Coalson and A. Duncan, J. Chem. Phys. **97**, 5653 (1992).
[18] W. H. Press, B. P. Flannery, S. A. Teukolsky, and W. T. Vetterling, *Numerical Recipes in C: The Art of Scientific Computing* (Cambridge University Press, Cambridge, 1992).
[19] S. Tsonchev, R. D. Coalson, and A. Duncan, Phys. Rev. E **60**, 4257 (1999).
[20] D. Frenkel, G. C. A. M. Mooij, and B. Smith, J. Phys.: Condens. Matter **4**, 3053 (1992).
[21] A. Brandt, Math. Comput. **31**, 333 (1977).
[22] T. L. Beck, Int. J. Quantum Chem. **65**, 477 (1997).
[23] Y. A. Rozanov, *Probability Theory: A Concise Course* (Dover, New York, 1969).
[24] T. Ambjörnsson, S. P. Apell, Z. Konkoli, E. A. Di Marzio, and J. J. Kasianowicz, J. Chem. Phys. **117**, 4063 (2002); M. Muthukumar, *ibid.* **118**, 5174 (2003).